

## Metastability of the uniform magnetization in three-dimensional random-field Ising model systems. II. $\text{Fe}_{0.47}\text{Zn}_{0.53}\text{F}_2$

P. Pollak and W. Kleemann

*Angewandte Physik, Universität Duisburg, D-4100 Duisburg 1, Federal Republic of Germany*

D. P. Belanger

*Department of Physics, University of California, Santa Cruz, California 95064*

(Received 7 March 1988)

Optical Faraday rotation was used to measure the uniform magnetization  $M$  versus temperature  $T$ , field  $H$ , and time  $t$  of the random-field Ising model system  $\text{Fe}_{0.47}\text{Zn}_{0.53}\text{F}_2$ . The critical behavior of  $(\partial M/\partial T)_H$  versus  $T$  in fields up to 5 T confirms previous results at lower fields  $H \leq 1.9$  T. The dynamical rounding temperature  $\varepsilon^*$  scales as  $H^{2/\phi}$  with  $\phi \sim 1.4$ , as predicted previously. Excess magnetization  $\Delta M$  is found in the field-cooled or field-decreased metastable domain state, respectively.  $\Delta M$  is concentrated at the domain walls and, hence, scales as  $H^2$  at  $T \sim T_c(H)$ . On cooling  $\Delta M$  approaches zero in the low- $H$ , broad-wall limit, but  $\Delta M$  is approximately constant for large  $H$  at all  $T < T_c(H)$ , where vacancy pinning dominates. By decreasing from large  $H$  at constant low  $T$ , one subsequently finds  $\Delta M \propto [T \ln(t/\tau)]^{-1}$ . Both the behavior for  $T \sim T_c$  and for high  $H$  are essentially as predicted recently by Nattermann and Vilfan. The primary difference is that  $\tau$  is not simply a constant attempt time,  $\tau_0 \sim 10^{-14} - 10^{-10}$  s, but rather varies with  $T$ , approximately as  $\tau = \tau_0 \exp(DT)$ , with  $D \sim 1.3 \text{ K}^{-1}$ . This can be understood by considering the increasing influence of domain volume contributions to  $\Delta M$  as  $T$  approaches  $T_c$ .  $\Delta M > 0$  is also found on reversing the  $T$  scan of a zero-field cooled sample below but close to  $T_c$ .  $\Delta M$  in this case is due to the freezing-in of very slow finite-size thermal fluctuations and does not indicate broken long-range order.

### I. INTRODUCTION

Random-field Ising-model (RFIM) systems,<sup>1</sup> as realized by dilute anisotropic antiferromagnets in a uniform external magnetic field (DAFF),<sup>2</sup> are well known<sup>3</sup> to evolve metastable microdomain structures, if the low-temperature state is achieved via field-cooling (FC). Since the ground state in  $d = 3$  dimensions has long-range order (LRO),<sup>4</sup> the average domain radius,  $R$ , might be expected to grow in time. Because of domain-wall pinning at local random-field (RF) fluctuations, weak, viz. logarithmic, time dependence has been predicted.<sup>5-7</sup>

Additional pinning arises in DAFF systems, however, owing to fluctuations of their random-bond (RB) distribution.<sup>8</sup> It can be shown<sup>9</sup> that RB pinning is most effective in systems with strong anisotropy, hence exhibiting narrow domain walls. At low temperatures these are fixed at the positions determined by the FC process, irrespective of any changes of the RF. Indeed, from neutron scattering experiments it is well known that the FC domain configuration is frozen at low temperatures, even if the external field is switched off.<sup>10</sup> Computer simulations<sup>11</sup> yield essentially the same result.

Recently, measurements of the uniform magnetization,  $M$ , provided valuable information on RF induced domain states in DAFF systems like  $\text{Mn}_x\text{Zn}_{1-x}\text{F}_2$ ,<sup>12</sup> and  $\text{Fe}_x\text{Mg}_{1-x}\text{Cl}_2$ .<sup>13</sup> In agreement with computer experiments,<sup>11</sup> the formation of antiferromagnetic domains implies an enhancement of  $M$ . This is quite evident from  $M$  versus  $T$  cycles around  $T_c(H)$  at constant field  $H$ , starting

well below  $T_c(H)$  after zero-field cooling (ZFC). It was argued<sup>13</sup> that the excess magnetization,  $\Delta M = M_{\text{FC}} - M_{\text{ZFC}}$ , is mainly stored in the domain walls. In these interfaces, which take advantage of extended clusters of missing bonds, favorable spins are readily aligned with  $H$ .<sup>14</sup> Assuming a constant surface density of favorable spins,<sup>13</sup> one easily obtains  $\Delta M \propto R^{-1}$ . Since  $R^{-1}$  is proportional to  $H^{2,5,7}$  the relation  $\Delta M \propto H^2$  should hold. On the experimental side this was indeed verified for  $\text{Fe}_{0.7}\text{Mg}_{0.3}\text{Cl}_2$  at temperatures just below  $T_c(H)$ .<sup>13</sup> On the other hand, in a more elaborate theoretical consideration taking into account fractality of the interfaces on small length scales, Nattermann and Vilfan recently<sup>9</sup> arrived at the same conclusion.

In a preceding paper<sup>15</sup> (henceforth referred to as I) we studied the metastability properties of  $\text{Fe}_{0.7}\text{Mg}_{0.3}\text{Cl}_2$  in more detail. Emphasis was put onto the temperature regimes where the FC induced domains are believed<sup>7,9</sup> to be either frozen in [ $T \ll T_c(H)$ ] or rapidly relaxing [ $T \lesssim T_c(H)$ ]. At low temperatures we studied the remanent magnetization,  $\mu$ , in the absence of RF after switching off the field  $H$ . Logarithmically slow temporal decay was found, which can be explained<sup>9</sup> by RB controlled spin readjustment within the domain walls. Domain size relaxation becomes important only in the vicinity of  $T_c(H)$ . This is evident, e.g., from the decrease of  $\Delta M$  with  $T$  observed during FC close to  $T_c(H)$ .

Most surprisingly, we also found irreversibilities within  $M$  versus  $T$  cycles at  $T < T_c(H)$  in the ZFC configuration. Excess magnetization,  $\Delta M > 0$ , appears upon FC when

reversing the temperature *very close* to but *below*  $T_c(H)$ . This is attributed to frozen-in short-range order-parameter fluctuations in the range of extreme RFIM critical slowing down.<sup>3,7,16</sup>

In the present paper the above described investigations<sup>15</sup> are extended to the strongly anisotropic DAFF system  $\text{Fe}_x\text{Zn}_{1-x}\text{F}_2$ . The primary purpose was to confirm that irreversibility of  $M$  is neither merely a structural peculiarity of the system under investigation ( $\text{Fe}_x\text{Mg}_{1-x}\text{Cl}_2$  has a layered structure with preponderant quasi-2D ferromagnetic interactions), nor just connected with weak anisotropy as in the case of  $\text{Mn}_x\text{Zn}_{1-x}\text{F}_2$ .<sup>12</sup> Indeed, corresponding  $\Delta M$  effects arise very clearly also in the "standard" system  $\text{Fe}_x\text{Zn}_{1-x}\text{F}_2$ . Their relative magnitudes are similar to those reported in I.

In addition to isomagnetic cycles,  $M$  versus  $T$ , as performed in I, we also measured isothermal field cycles,  $M$  versus  $H$ , thus crossing the  $H$ - $T$  phase boundary on paths parallel to the  $H$  axis. Again, domain states with enhanced magnetization are clearly observed. Moreover, we studied the time dependence of  $\Delta M$  after isothermally decreasing the field to a finite value,  $H_f \neq 0$ . Similarly as observed in  $\text{Fe}_{0.7}\text{Mg}_{0.3}\text{Cl}_2$  for  $H_f = 0$ ,<sup>15</sup> a logarithmic decay law emerges. At low  $T$  this may, again, be discussed in terms of RB controlled domain-wall relaxation.

The magnetization data are taken with the Faraday rotation technique<sup>17</sup> on a sample of  $\text{Fe}_{0.47}\text{Zn}_{0.53}\text{F}_2$  in fields up to  $H = 5$  T. Since previous measurements on this sample were limited to  $H \leq 1.9$  T,<sup>17</sup> we present also some critical data,  $(\partial M / \partial T)_H$  versus  $T$ , obtained after ZFC at these higher fields. On one hand, it is interesting to confirm the logarithmic divergence<sup>17</sup> also within  $1.9 \text{ T} \leq H \leq 5 \text{ T}$ . On the other hand, the data reveal the growing importance of dynamical rounding<sup>17,18</sup> in the higher-field region. As in the case of  $\text{Fe}_{0.7}\text{Mg}_{0.3}\text{Cl}_2$ ,<sup>15</sup> we argue that this is intimately connected with the occurrence of excess magnetization upon reversing  $T$  very close to  $T_c$  in the ZFC configuration.

## II. EXPERIMENTAL PROCEDURE

All experiments were done on the same sample of  $\text{Fe}_{0.47}\text{Zn}_{0.53}\text{F}_2$  as was used in the former study<sup>17</sup> and with the apparatus and technique described previously.<sup>13,15</sup> By using a narrow HeCd laser beam (diameter  $\sim 0.6$  mm,  $\lambda = 442$  nm), directed rather precisely along the  $c$  axis (thickness 3.0 mm), which is perpendicular to the concentration gradient, the gradient induced rounding of the phase transition is estimated to be no larger than  $\delta\varepsilon = 5 \times 10^{-4}$ . Temperatures were stabilized to within  $\delta T = 2$  mK. The FR rotation angle,  $\theta$ , was resolved with an accuracy of  $\delta\theta = 0.006^\circ$ .

The experimental results are interpreted by assuming strict proportionality of the FR with the magnetization  $M$ .<sup>17</sup> Support of this view is lent by measurements of the spectral dispersion of the FR of pure  $\text{FeF}_2$  in the extended range  $325 \text{ nm} \leq \lambda \leq 633 \text{ nm}$ . The typical<sup>17</sup>  $\lambda^{-2}/(\lambda_0^{-2} - \lambda^{-2})$  dependence is clearly confirmed with  $\lambda_0 = 154$  nm.

Owing to the nonergodic behavior of  $M$  in the vicinity of  $T_c(H)$ , a well-defined protocol has to be obeyed in any

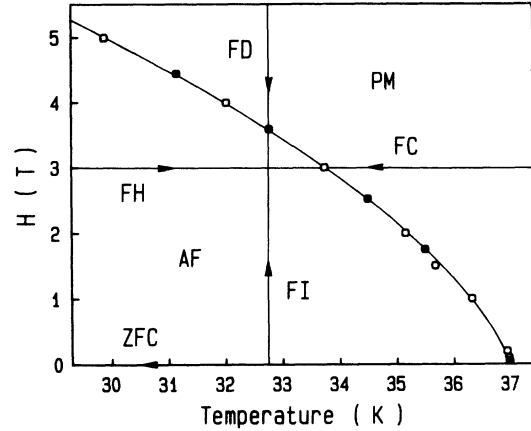


FIG. 1.  $H$  vs  $T$  phase diagram of  $\text{Fe}_{0.47}\text{Zn}_{0.53}\text{F}_2$  as determined from the divergences of  $(\partial\theta/\partial T)_H$  (open circles) and  $(\partial\theta/\partial H)_T$  (solid circles) for  $0 \leq H \leq 5$  T. Straight lines with arrows, crossing the interpolated AF-PM phase line, indicate the measurement routines, ZFC, FC, FH, FD, and FI (see text).

measurement. Different standard procedures used to cross the para-to-antiferromagnetic phase line of  $\text{Fe}_{0.47}\text{Zn}_{0.53}\text{F}_2$  are schematically shown in Fig. 1. Isotherms may be recorded either by FC or by FH. The latter procedure may be preceded by ZFC. Isotherms are taken by either field increasing (FI) or by field decreasing (FD).

## III. EXPERIMENTAL RESULTS

Figure 2 shows the temperature dependence of  $(\partial\theta/\partial T)_H$  taken after ZFC upon FH at various fields,  $H = 1, 1.5, 2, 3, 4,$  and  $5$  T (curves 1–6, respectively). The data referring to  $H = 1$  and  $1.5$  T agree with those obtained previously,<sup>17</sup> except for an upward shift by  $0.52$  K of the  $T$  scale, presumably due to calibration errors. As typically observed,<sup>17</sup> the peaks are symmetric and shift to lower  $T$  upon increasing  $H$ . A semilogarithmic plot,  $(\partial\theta/\partial T)_H$  versus  $\log_{10} |\varepsilon|$ , where  $\varepsilon = (T - T_c)/T_N$ ,

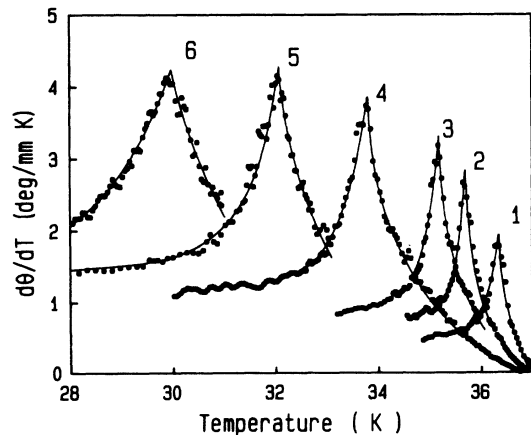


FIG. 2.  $(\partial\theta/\partial T)_H$  vs  $T$  for zero-field cooled  $\text{Fe}_{0.47}\text{Zn}_{0.53}\text{F}_2$  measured at  $H = 1, 1.5, 2, 3, 4,$  and  $5$  T (curves 1–6, respectively) and  $\lambda = 442$  nm. The solid lines are guides for the eye.

reveals linearity over about one decade of  $|\varepsilon|$  for each field (Fig. 3).

The values of  $T_c(H)$  were obtained by optimizing the data collapsing in Fig. 3 at both  $\varepsilon > 0$  and  $\varepsilon < 0$ . They are plotted as  $H$  versus  $T_c(H)$  in Fig. 1, including low-field data referring to  $H=0.05, 0.1$ , and  $0.2$  T (open circles).  $T_c(H)$  obeys crossover scaling, i.e.,  $T_c(H) = T_N - aH^{2/\phi} - bH^2$ , where  $a$  and  $b$  are constants and  $\phi$  is the crossover exponent from random-exchange Ising model (REIM) to RFIM behavior. Applying the mean-field correction,  $bH^2$ , in the manner previously described,<sup>17</sup> we obtain  $\phi = 1.40 \pm 0.05$  in good agreement with the now widely accepted best value  $\phi = 1.42 \pm 0.03$ .<sup>3</sup> Note that the Néel temperature,  $T_N = 36.98$  K, was obtained from the best-fit procedure used to determine  $\phi$ .

Obviously, the  $(\partial\theta/\partial T)_H$  peaks (Fig. 2) are widening

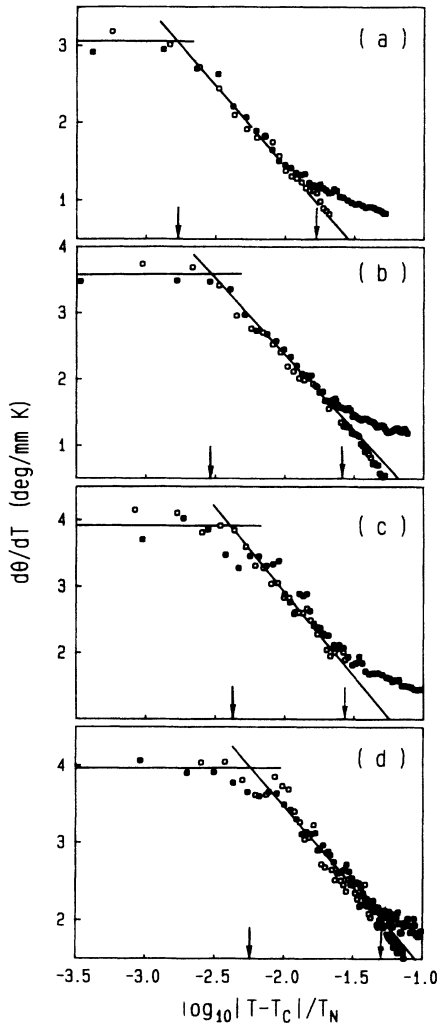


FIG. 3.  $(\partial\theta/\partial T)_H$  vs  $\log_{10}|\varepsilon|$  for  $H=2, 3, 4$ , and  $5$  T [curves (a)–(d), respectively], where  $\varepsilon = [T - T_c(H)]/T_N$  with  $T_N = 36.98$  K and  $T_c = 35.16$  K (a),  $33.74$  K (b),  $32.02$  K (c), and  $29.88$  K (d). Solid (open) circles refer to  $\varepsilon < 0$  ( $\varepsilon > 0$ ). The right- and left-hand arrows, respectively, denote the  $|\varepsilon|$  values referring to REIM-RFIM crossover and to dynamical critical rounding, respectively (see text).

at increasing  $H$ . This is due to the extension of the RFIM regime towards larger  $|\varepsilon|$ . The REIM-to-RFIM crossover temperature, at which the branches referring to  $\varepsilon > 0$  and  $\varepsilon < 0$  in the semilog plot of Fig. 3 separate, is shifting from  $|\varepsilon| \sim 0.016$  to  $|\varepsilon| \sim 0.063$  when increasing  $H$  from  $2$  to  $5$  T (right-hand arrows in Fig. 3).

On the other hand, the  $(\partial\theta/\partial T)_H$  curves become increasingly rounded with increasing  $H$ . This is due to the tremendous critical slowing down of the RFIM.<sup>16</sup> It occurs within the region near  $T_c(H)$  described by the “dynamical rounding temperature,”  $\varepsilon^*$ ,<sup>17,18</sup> which is defined by the intersection of the asymptotic  $\ln|\varepsilon|$  behavior of the singularity with a horizontal line through the peak height at  $|\varepsilon| = 0$  in a semilogarithmic plot.  $\varepsilon^*$  is, of course, largely dependent on the timescale of the experiment<sup>17,18</sup> (here  $\tau \sim 25$  s). It has recently been argued<sup>19</sup> that, for fixed  $\tau$ , the width of the rounding should scale as  $T_c(H)$ , i.e.,  $\varepsilon^* \propto H^{2/\phi}$ . Indeed, the values obtained from Fig. 3 (left-hand arrows),  $\varepsilon^* = 1.7, 2.9, 4.1$ , and  $5.8 \times 10^{-3}$  for  $H = 2, 3, 4$ , and  $5$  T, respectively, are well described by this power law with  $\phi = 1.49 \pm 0.10$ . This result agrees with the preceding “best”  $\phi$  value, albeit bearing a relatively large error due to uncertainties in determining the correct  $\varepsilon^*$  values.

The amplitude of the logarithmic divergence of  $(\partial\theta/\partial T)_H$  is expected<sup>17</sup> to obey a  $H^y$  dependence, where  $y = 2(1 + \bar{\alpha} - \alpha - \phi/2)/\phi \sim 0.54$ , inserting the RFIM and REIM exponents  $\bar{\alpha} = 0$  and  $\alpha = -0.09$ , respectively, and  $\phi = 1.42$ . Our data taken from Fig. 3 at  $|\varepsilon| = 0.01$  yield  $y = 0.7 \pm 0.1$ , in rough agreement with the expected value. The error bars mainly reflect the ambiguity in properly subtracting the noncritical background.

Figure 4(a) shows original  $\theta$  versus  $T$  data, taken upon FH at  $H = 4$  T after ZFC (curve 1). The logarithmic divergence of the derivative,  $(\partial\theta/\partial T)_H$  (Fig. 2, curve 5) is clearly indicated by the inflection point at  $T_c = 32.02$  K. Upon reversing  $T$  at  $33.0$  K and subsequent FC, however,  $\theta$  versus  $T$  flattens appreciably, such that  $\theta_{FC} > \theta_{ZFC}$  (curve 2). Hence, excess FR,  $\Delta\theta = \theta_{FC} - \theta_{ZFC} > 0$ , appears similarly as in  $\text{Mn}_x\text{Zn}_{1-x}\text{F}_2$  (Ref. 12) and  $\text{Fe}_{0.7}\text{Mg}_{0.3}\text{Cl}_2$ .<sup>13,15</sup> It starts to grow at  $T \sim T_{eq} = 32.85$  K, has its steepest increase at  $T_c$  and reaches a flat maximum,  $\Delta\theta_m$ , at  $T_m = 31.10$  K. As a rule, one finds  $\varepsilon_m \sim -\varepsilon_{eq}$ , a result similar to that observed previously.<sup>13</sup> Another analogy with the  $\text{Fe}_{0.7}\text{Mg}_{0.3}\text{Cl}_2$  system is the proportionality of  $\Delta\theta_m$  with  $H^2$  as shown in the inset of Fig. 5.

The decrease of  $\Delta\theta$  for  $T < T_m$  is most pronounced in the low- $H$  limit, where  $\Delta\theta$  essentially vanishes at low enough  $T$  (Fig. 5, curve 1). Evidently the ZFC ground state is achieved in case that the domain walls are pinned by small enough RF. At sufficiently large RF, however, the FC domain state becomes completely frozen in as  $T$  is decreased. At  $H = 5$  T we observe constant  $\Delta\theta \sim \Delta\theta_m$  at whatever temperature,  $T < T_m$  (Fig. 5, curve 4).

Further decrease of  $\Delta\theta$  is found upon FH after FC. This is shown for  $H = 4$  T in Fig. 4(b) (open circles) after reversing  $T$  at  $27.0$  K. Within the range  $0.84 \leq T/T_c \leq 0.98$ ,  $\Delta\theta$  decreases linearly with  $T$  by about 25%. The remaining signal is close to that obtained upon

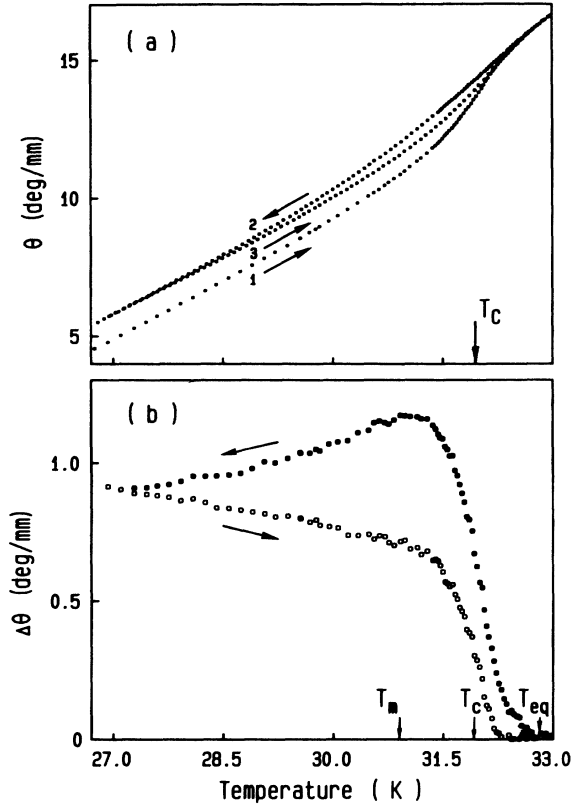


FIG. 4. (a)  $\theta$  vs  $T$  measured after ZFC at  $H=4$  T and  $\lambda=442$  nm upon FH (curve 1), FC (2), and FH, again (3), as indicated by arrows. (b) Differences  $\Delta\theta$  vs  $T$  of curves 2 (solid circles) and 3 (open circles) with curve 1 of (a).  $T_m$ ,  $T_c$ , and  $T_{eq}$  are indicated by arrows (see text).

FC with  $H=3$  T (Fig. 5, curve 2). Hence, during the FC-FH cycle the system has relaxed toward a domain state corresponding to a *smaller* field. Indeed, in the critical region,  $0.98 \leq T/T_c \leq 1.02$ , the rapid decay of the FH curve at  $H=4$  T maps rather precisely onto the FC curve referring to  $H=3$  T. Note that the temperature

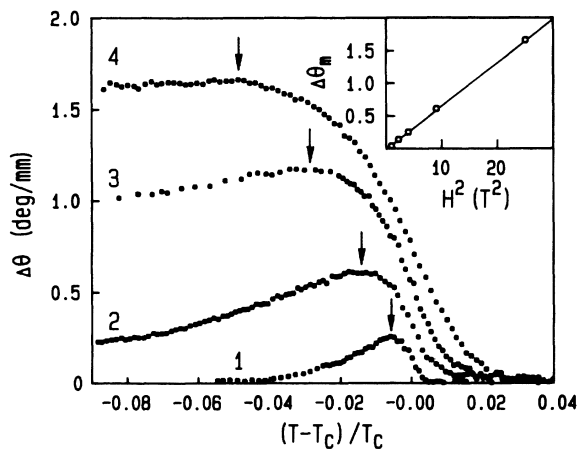


FIG. 5.  $\Delta\theta = \theta_{FC} - \theta_{ZFC}$  vs  $(T - T_c)/T_c$ , measured at  $\lambda=442$  nm and  $H=2, 3, 4$ , and  $5$  T (curves 1–4, respectively). For the  $T_c$  values see Fig. 3.  $T_m$  values are indicated by arrows. The inset shows  $\Delta\theta_m = \Delta\theta(T_m)$  vs  $H^2$ .

range for building up the FC state at  $H=4$  T is significantly larger,  $0.97 \leq T/T_c \leq 1.03$ , than that for its rapid decay.

A novel feature, already reported in I for  $\text{Fe}_{0.7}\text{Mg}_{0.3}\text{Cl}_2$ , is the appearance of excess FR,  $\Delta\theta > 0$ , in the ZFC ground state after reversing the ZFC-FH scan (curve 1) at  $T_r=31.75$  K ( $\epsilon_r = -0.007$ ). This is shown for  $H=4$  T in Fig. 6. Subsequent FC clearly induces enhanced FR,  $\Delta\theta > 0$  (curve 2). Upon decreasing  $|\epsilon_r|$ , i.e.,  $T_r \rightarrow T_c$ ,  $\Delta\theta$  increases, albeit remaining small compared with the maximum  $\Delta\theta$  effect, which arises after FC from above  $T_{eq}=32.85$  K (Fig. 6, curve 3). On the other hand, the lowest  $T_r$  allowing for clear observation of  $\Delta\theta$  ( $\geq 5\%$  of maximum  $\Delta\theta$ ), decreases upon increasing  $H$ . Essentially,  $\epsilon_{r,\min}$  seems to vary with  $H$  like the dynamical rounding temperature  $\epsilon^*$  (Fig. 3). Within the range  $2 \text{ T} \leq H \leq 5 \text{ T}$  we find  $|\epsilon_{r,\min}| \sim 1.7\epsilon^*$ . This relation is relevant to the discussion below.

Excess FR is also observed in *isothermal* field scans at  $T < T_N$ . First of all,  $\theta$  versus  $H$  recorded at constant  $T$  after ZFC upon FI resembles very much the more familiar  $\theta$  versus  $T$  isomagnets (Figs. 4 and 6) in the critical region, i.e.,  $H \sim H_c(T)$  or  $T \sim T_c(H)$ . This is shown by the FI curve taken at  $T=32.77$  K in Fig. 7(a) (open circles). It exhibits a point of inflection at  $H_c=3.59$  T. The corresponding peak of  $(\partial\theta/\partial H)_T$  versus  $H$  (Fig. 7(b), open circles) resembles that of  $(\partial\theta/\partial T)_H$  versus  $T$  (Fig. 2). Analysis (not shown) reveals a symmetrical logarithmic divergence,  $(\partial\theta/\partial H)_T \propto \ln|h|$ , within  $0.02 \leq |h| \leq 0.07$ , where  $h = (H - H_c)/H_c$ . Rounding and splitting of the branches are found at  $|h| < 0.02$  and  $> 0.07$ , respectively. Indeed, the critical behavior described by<sup>17</sup>  $(\partial\theta/\partial H)_T \propto H^y \ln|\epsilon|$  can be shown to contain a leading  $\ln|h|$  contribution under isothermal conditions. Hence, a semilogarithmic plot versus  $\ln|h|$  yields correct  $H_c(T)$  values, which fit nicely with the  $H$  versus  $T$  phase diagram (Fig. 1, solid circles). However, as remarked previously,<sup>20</sup> the complicated relationship  $\epsilon = \epsilon(h)$  (see above) makes isotherms,  $(\partial\theta/\partial H)_T$  versus  $H$ , unsuitable

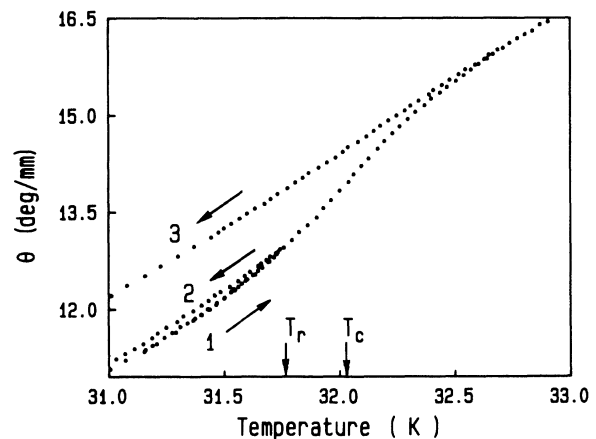


FIG. 6.  $\theta$  vs  $T$  at  $H=4$  T and  $\lambda=442$  nm, measured after ZFC upon FH (curve 1), FC at  $T \leq T_r=31.75$  K (2), and FC at  $T \leq 33.0$  K (3), respectively.  $T_r$  and  $T_c=32.02$  K are indicated by arrows.

for critical point analysis.

Here we focus upon irreversibility effects. They are readily found upon FD after reversing the field scan at  $H > H_c$  [Fig. 7(a), solid circles]. Very clearly,  $\theta_{FD} > \theta_{FI}$  in the vicinity of  $H_c$ , where the curvature of  $\theta$  versus  $H$  is very much reduced and the peak of  $(\partial\theta/\partial H)_T$  versus  $H$  flattens appreciably [Fig. 7(b), solid circles]. At low fields,  $H \lesssim 2$  T, both  $\theta_{FD}$  and  $\theta_{FI}$  merge into one another, hence,  $\Delta\theta = \theta_{FD} - \theta_{FI} \rightarrow 0$ . This is common to all isotherms studied here under the constraint  $H_c(T) \leq 5$  T (Fig. 1). Figure 8 shows  $\Delta\theta$  versus  $H$ , measured at  $T = 35.5$  K (curve 1), 34.5 K (2), 32.77 K [3; cf. Fig. 7(a)] and 31.15 K (4) with corresponding  $H_c$  values of 1.75, 2.52, 3.56, and 4.45 T, respectively (cf. Fig. 1).

It is seen that  $\Delta\theta$  starts to grow on FD below  $H_{eq} > H_c(T)$  and peaks at  $H_m < H_c(T)$ .  $H_{eq}$  and  $H_m$  are analogous to  $T_{eq}$  and  $T_m$  as obtained from isomagnetic  $\theta$  versus  $T$  curves (Fig. 5). Analysis (not shown) reveals  $h_{eq} \sim -h_m \sim 0.07$  in all cases shown in Fig. 8, whereas the peak values,  $\Delta\theta_m$ , scale approximately as  $H_m^2$ . This reminds us of the relation  $\Delta\theta_m \propto H_m^2$ , observed on isomagnets (Fig. 5, inset). The decrease of  $\Delta\theta$  as  $H \rightarrow 0$  is certainly due for the most part to the decrease of the RF. Remanence,  $\Delta\theta(H=0)$ , will be vanishingly small, since all  $T$  chosen in Fig. 8 are very close to  $T_N$ . As pointed

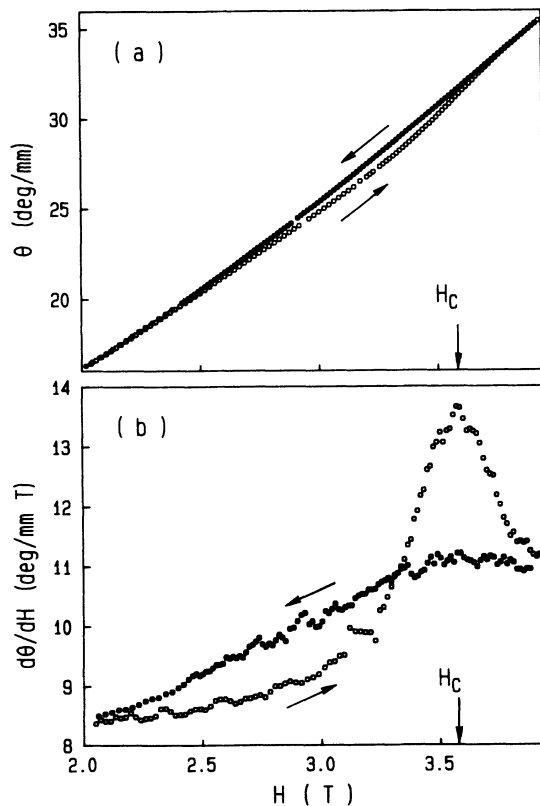


FIG. 7.  $\theta$  vs  $H$  (a) and  $(\partial\theta/\partial H)_T$  vs  $H$  (b) measured at  $T = 32.77$  K and  $\lambda = 442$  nm after ZFC upon FI (open circles) and subsequent FD (solid circles), respectively.  $H_c = 3.56$  T is indicated by arrows.

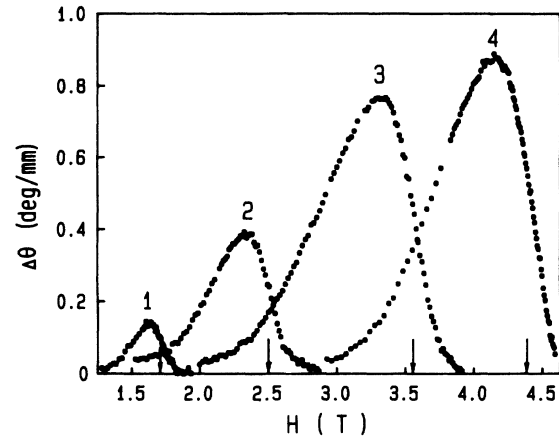


FIG. 8.  $\Delta\theta = \theta_{FD} - \theta_{FI}$  vs  $H$ , measured at  $\lambda = 442$  nm and  $T = 35.5$  K (curve 1), 34.5 K (2), 32.77 K [3; see Fig. 7(a)] and 31.15 K (4), respectively. The corresponding values  $H_c = 1.75$ , 2.52, 3.56, and 4.45 T, respectively, are indicated by arrows.

out in I, at  $T \geq 0.8T_N$  essentially instantaneous domain growth towards LRO is expected for  $H \rightarrow 0$ .

Observation of remanence effects upon FD requires low temperatures, where the domains are essentially immobile.<sup>10,11</sup> However, the ZFC-FI-FD procedure as chosen for Figs. 7 and 8 is inapplicable for experimental reasons, since  $H_c > 5$  T at  $T < 30$  K. More appropriately,<sup>15</sup> the domain state can be prepared by FC in a large field,  $H_0$ . Then the excess FR and/or remanence may be studied after isothermal FD to a field  $H < H_0$ .

Figure 9 shows two differently prepared  $\theta$  versus  $T$  curves measured upon FH at  $H = 2$  T. Curve 1 refers to ZFC prior to applying  $H$  at  $T = 10$  K. Curve 2 was recorded after FC at  $H_0 = 5$  T from  $T = 40$  to 12 K and subsequent isothermal FD to  $H = 2$  T. Surprisingly, the difference of the two curves,  $\Delta\theta$  versus  $T$ , differs strongly from that corresponding to FC at  $H = 2$  T (Fig. 5, curve 2). Whereas in the latter case  $\Delta\theta$  vanishes as  $T < 0.96T_c(2T) = 33.75$  K, the novel FC-FD cycle yields

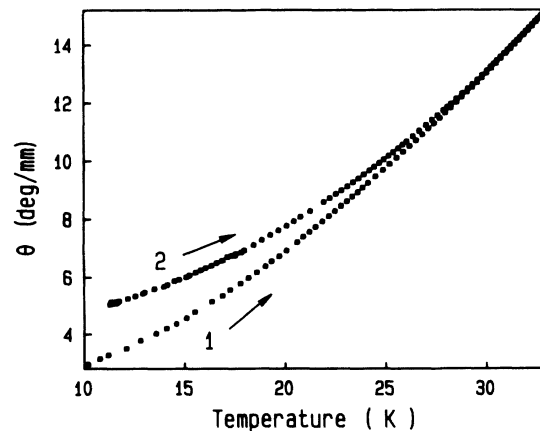


FIG. 9.  $\theta$  vs  $T$  measured upon FH at  $\lambda = 442$  nm and  $H = 2$  T after ZFC (curve 1) and after FC from  $T = 40$  to 12 K at  $H_0 = 5$  T and subsequent FD to  $H = 2$  T (curve 2), respectively.

very large low- $T$  values of  $\Delta\theta$ . At  $T=12$  K we find  $\Delta\theta\sim 1.6$  deg/mm, i.e., the same value as frozen in upon FC with  $H_0=5$  T at  $T\lesssim T_c$  (Fig. 5, curve 4). Evidently, we are able to preserve the FC-FD domain configuration for all temperatures  $T < T_c$  at the lower field. In the measurement of Fig. 9 this state is exposed to increasing temperatures in the reduced field,  $H < H_0$ . Within  $12$  K  $\leq T \leq 20$  K,  $\Delta\theta$  decreases approximately as  $T^{-1}$ , but the decrease is much stronger at higher  $T$  until it vanishes at  $T\sim 30$  K. This might hint at time dependence and domain growth effects<sup>15</sup> in addition to the pure  $T$  dependence of the domain-wall relaxation.<sup>9</sup>

It is, hence, useful to measure  $\Delta\theta$  versus  $t$  at fixed temperatures,  $T$ , after preparing the initial domain state in the same way as described above. Figure 10 shows some isotherms thus obtained within  $15.7$  K  $\leq T \leq 31.1$  K. Indeed, all of these curves exhibit temporal decay, starting rapidly at  $t=0$  and yielding a nearly constant tail at  $t > 1000$  s. Note that  $t=0$  refers to the *beginning* of the FD from  $H_0$  to  $H$ . Hence, data points are lacking at  $t < 45$  s, the time required to lower the field. The first rapid decrease, starting at  $\Delta\theta(0)\sim 1.6$  deg/mm at *all* temperatures, unfortunately remains uncharacterized.

In contrast to the procedure used to obtain the data shown in Fig. 9, we are now able to analyze  $\Delta\theta$  versus  $T$  data at well-defined times. Choosing e.g.,  $t=1500$  s in Fig. 10, we may describe the  $T$  dependence in the *entire* range  $15$  K  $\leq T \leq 28$  K as

$$\Delta\theta/(\text{deg/mm})=41.9 \text{ K}/T-1.42. \quad (1)$$

This phenomenological equation is a compromise between the  $T^{-\psi}$  law expected<sup>9,15</sup> at low  $T$  ( $\psi\sim 1$ ) and the requirement that  $\Delta\theta\rightarrow 0$  as  $T\rightarrow T_c^-$ . One obtains  $T_c^-=29.4$  K, which is not too far from the correct value,  $T_c=35.16$  K. At  $T > 29.4$  K Eq. (1) becomes meaningless and should be replaced by  $\Delta\theta=0$ . This is compatible with both  $\Delta\theta$  versus  $t$  at  $t > 300$  s for  $T=31.1$  K (Fig. 10, curve 6) and  $\Delta\theta$  versus  $T$  upon FC in  $H=2$  T at  $T < 33.8$

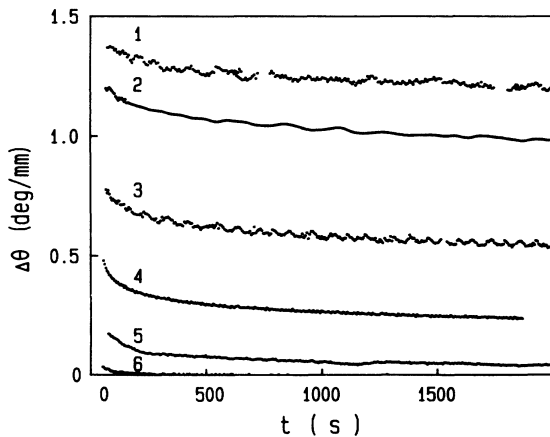


FIG. 10. Time dependence of the excess FR, produced by FC (5 T) followed by FD (2 T) (see Fig. 9) at constant temperatures  $T=15.7$  K (curve 1),  $17.4$  K (2),  $21.3$  K (3),  $24.75$  K (4),  $27.5$  K (5), and  $31.1$  K (6), respectively. Experimental noise is mainly caused by  $T$  instability.

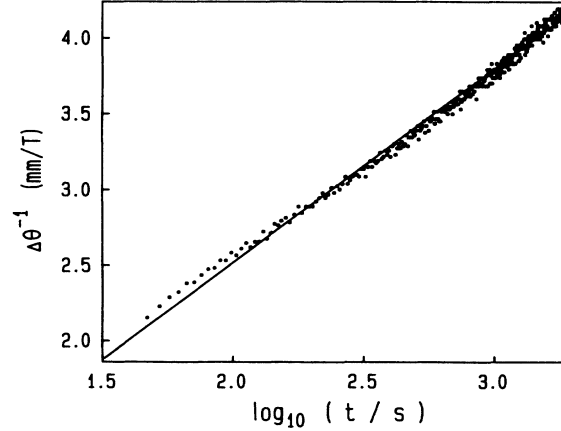


FIG. 11.  $\Delta\theta^{-1}$  vs  $\log_{10}(t/s)$ , measured at  $T=24.75$  K (see Fig. 10, curve 4). The straight line is the best fit of the data points to Eq. (2).

K (Fig. 5, curve 1).

The temporal decay of the excess FR is reasonably well described by

$$\Delta\theta=\Delta\theta_0 \ln(t/\tau)^{-1}. \quad (2)$$

Indeed, by plotting, e.g., the  $T=24.75$  K data (Fig. 10, curve 4) as  $\Delta\theta^{-1}$  versus  $\log_{10}(t/s)$  in Fig. 11, one obtains a reasonably straight line. A best fit to Eq. (2) yields the time constant  $\tau=1.3$  s. The other isotherms of Fig. 10 behave similarly, albeit exhibiting a systematic increase of  $\tau$  with increasing  $T$ :  $\tau(15.7\text{K})\sim 10^{-7}$  s,  $\tau(17.4\text{K})=3.4\times 10^{-5}$  s,  $\tau(21.3\text{K})=1.8\times 10^{-2}$  s, and  $\tau(27.5\text{K})=26.2$  s. This result looks inconsistent with current theories,<sup>9</sup> which consider  $\tau$  to be a constant microscopic attempt time to overcome local energy barriers, with  $\tau\sim 10^{-14}-10^{-10}$  s. In the discussion (Sec. IV A) it will be shown how to resolve this discrepancy.

## IV. DISCUSSION

### A. Low-temperature relaxation

Following the previous discussion,<sup>15</sup> highly anisotropic DAFF are characterized by essentially immobile antiferromagnetic domains at low  $T$ .<sup>10</sup> Their average radius is mainly determined by the field  $H_0$  applied during FC,  $R\propto H_0^{-2}$ .<sup>5-7</sup> The cooling rate through  $T_c$  may have a measurable influence, as well.<sup>15</sup> The domain walls store excess magnetization,<sup>13,14</sup>  $\Delta M\propto R^{-1}$ , which causes most of the experimentally found excess FR,  $\Delta\theta$ .

Upon decreasing the external field at low  $T$ , the domain walls remain pinned by RB fluctuations.<sup>9</sup> RF merely control the spin readjustments of the interfaces on small scales. These give rise to a temporal decrease of the surface magnetization<sup>9</sup>

$$\Delta M_s(t, T)=AH_0^2[T \ln(t/\tau_0)]^{-\psi}, \quad (3)$$

where  $A$  is a constant,  $\psi\sim \frac{2}{3}$ , and  $\tau_0$  denotes a microscopic relaxation time,  $\tau_0=10^{-14}-10^{-10}$  s.

Another contribution to  $\Delta M$  is due to the statistical excess of spins belonging to that sublattice, which is aligned with  $H_0$ . One expects an excess volume magnetization<sup>9</sup>

$$\Delta M_v = BH_0^3, \quad (4)$$

where the constant  $B$  should neither depend on  $t$  nor on  $T$ , provided that  $T \lesssim 0.8T_c$  (see the following).

Assuming  $\Delta M_v \ll \Delta M_s$ , which is certainly the case for large enough  $R$ , viz. small values of  $H_0$ , one may calculate from (3) and (4)

$$\begin{aligned} (\Delta M)^{-1} &= (\Delta M_s + \Delta M_v)^{-1} \sim \Delta M_s^{-1} (1 - \Delta M_v / \Delta M_s) \\ &= (T / AH_0^2) \ln(t / \tau_0) [1 - CH_0 T \ln(t / \tau_0)], \end{aligned} \quad (5)$$

where  $C = B / A$ . Here we set  $\psi = 1$  as determined from the  $T$  dependence of  $\Delta\theta$  [Eq. (1)]. Its deviation from the expected<sup>9</sup> value,  $\psi \sim 0.4$ , may be connected with still unknown structural properties of the interfaces. Equation (5) can be rewritten as

$$(\Delta M)^{-1} \sim (T / AH_0^2) \ln(t / \tau), \quad (6)$$

where

$$\tau = \tau_0 \exp[CH_0 T \ln^2(t / \tau_0)]. \quad (7)$$

Equation (6) describes the experimentally found linearity in  $T$  and the logarithmic  $t$  dependence of  $\Delta\theta^{-1}$  [Eqs. (1) and (2)]. Equation (7) explains the peculiar temperature dependence of  $\tau$  emerging from the fits. Indeed, our  $\tau$  versus  $T$  data reveal an exponential law,

$$\tau = \tau_0 \exp(DT), \quad (8)$$

with reasonable best-fit parameters  $\tau_0 = 0.4 \times 10^{-14}$  s and  $D = 1.34$  K<sup>-1</sup>. Putting  $t / \tau_0 = 10^{15} - 10^{17}$  and  $T = 20$  K, one obtains, by comparison with Eq. (6),  $\Delta M_s(t = \tau_0) / \Delta M_v \sim 45 - 60$ , where  $\Delta M_s(t = \tau_0) = AH_0^2 / T$ . Hence, the above assumption  $\Delta M_s \gg \Delta M_v$  obviously holds for our experiment, where the domain state was prepared with  $H_0 = 5$  T.

Closer inspection of Fig. 11 shows a slight increase of the slope of  $\Delta\theta^{-1}$  versus  $\log_{10}(t/s)$  for  $t \gtrsim 500$  s. This is positively *not* due to the neglect of the weak  $t$  dependence of  $\tau$  [Eq. (7)], which is rather expected to slow down the increase of  $\Delta\theta^{-1}$  at increasing  $t$  [see also Eq. (5)]. More probably, a secondary mechanism with higher attempt frequency, but lower efficiency than the domain-wall relaxation influences the decay of  $M$ . Probably this concerns domain *size* relaxation being non-negligible at  $T \sim 0.8T_c$ .<sup>15</sup> Hence, in order to test details of the theory of pure domain-wall relaxation, Eqs. (3)–(7), one should rather analyze data obtained at lower  $T$ , but with better signal-to-noise ratio than those of Fig. 10. In this context it will also be interesting to check the influence of RF pinning, which is expected to stop the spin relaxation after very long times provided that  $H \neq 0$ .

### B. Relaxation and pinning near $T_c(H)$

At temperatures very close to  $T_c(H)$  the domain walls in strongly anisotropic DAFF systems are broadened by thermal fluctuations. Hence,<sup>9</sup> the domain radius is determined by the RF,  $R \propto H^{-2}$ . This explains our result

$\Delta\theta_m \propto H^2$  (Fig. 5), neglecting small volume contributions proportional to  $H^3$  (see above). The gradual decrease of  $\Delta\theta$  upon FC below  $T_m$  [Fig. 4(b)] is compatible with the decrease of the RF, which is essentially proportional to  $M(T)/T$ .<sup>21</sup> Indeed, FC seems to be accompanied by domain growth as revealed by neutron scattering on  $\text{Fe}_{0.6}\text{Zn}_{0.4}\text{F}_2$  at  $H = 5.5$  T.<sup>22</sup> On subsequent FH, however, the domain radius was observed to remain constant.<sup>22</sup> The observed linear decrease of  $\Delta\theta$  on heating up to  $\sim 0.98T_c(H)$  [Fig. 4(b)] is, hence, very probably not due to domain growth. We are rather inclined to assume thermally induced spin readjustment of the otherwise immobile domain walls as described by Eq. (3).

The vanishing of  $\Delta\theta$  upon FC below  $T_m$  in the low-field limit (Fig. 5, curve 1) may be surprising. Obviously the ZFC ground state is achieved within finite time despite the nonvanishing RF due to nonzero applied field. On one hand, according to Villain,<sup>23</sup> this may reflect collective domain shrinkage due to broad-wall interaction. On the other hand, we also expect<sup>15</sup> temporal domain size relaxation for intermediate wall widths,<sup>9</sup> occurring at  $T \lesssim T_m$ . Curve 1 in Fig. 5 should thus depend on the cooling rate on measuring  $\theta_{\text{FC}}$ , an experiment which is still lacking. However, both mechanisms become ineffective in the strong RF limit, where narrow domain-walls emerge even close to  $T_c(H)$ . This explains why  $\Delta\theta$  remains nearly constant at  $T < T_m$  for  $H = 5$  T (Fig. 5, curve 4).

The appearance of excess FR in a ZFC sample when reversing a FH scan below  $T_c(H)$  (Fig. 6) might at first glance cast doubt on the ground-state nature of the DAFF system thus prepared. However, this effect is only observed in the temperature range where dynamical critical rounding occurs,  $|\epsilon_r| \lesssim 1.7\epsilon^*$ . Hence, the onset of metastability should closely be related to the drastic critical slowing down of the order-parameter fluctuations.<sup>16</sup> Presumably these are frozen on the time scale of the experimental changes in  $T$ , thus resembling static domain walls with inherent short-range disorder. Hence, upon cooling this disorder does not dissolve instantaneously, but rather remains pinned at the RF fluctuations, taking advantage of clusters of nonmagnetic ions.<sup>9,14</sup> In this way the system preserves memory of the less perfect AF order at some higher  $T$  and thus shows enhanced  $M$ . There is no a priori reason to believe that the frozen “domain walls” percolate. They rather resemble isolated clusters, which do not break LRO. Hence, the neutron Bragg peaks should still remain sharp despite the quasi-static inhomogeneity of the system. The existence of resolution limited Bragg peaks is indeed indicated by neutron scattering experiments on the same system for all  $T < T_c$  upon rising  $T$  after ZFC. Further details of this behavior are now under investigation in scattering experiments, including line shapes after reversing direction and cooling just below  $T_c$ .

### V. CONCLUSION

Excess magnetization,  $\Delta M > 0$ , characterizes the field induced domain state of the RFIM system  $\text{Fe}_{0.47}\text{Zn}_{0.53}\text{F}_2$ . In the low- $T$  limit the domains are immobile.<sup>10,11</sup> Relax-

ation upon FD at low  $T$  is, hence, restricted to the spins *within* the domain walls.<sup>9</sup> This is excellently confirmed by our experiments. Very reasonable agreement with theory is achieved, if the volume contributions to  $\Delta M$  are properly accounted for. The remaining discrepancy between the theoretical and the experimental values of the decay exponent  $\psi$  may eventually be resolved by both more elaborate analysis and additional experiments.

Rapid relaxation of the domain size upon decreasing the RF is most characteristic of the temperature range close to  $T_c(H)$ . Furthermore domain-wall interaction seems to favor relaxation toward LRO. Both mechanisms are connected with the appearance of broad domain walls and, apparently, do not operate at large enough RF. Unfortunately, a quantitative theory is not yet available.<sup>23</sup> In particular, whether or not time dependence may be observable in the broad-domain-wall regime is still an open question. Previous observations of time dependence in the vicinity of  $T_c(H)$  (Refs. 24 and 25) were very probably bound to relatively large RF, hence, narrow domain walls.

On the other hand, time dependence is very likely involved in the formation and the decay of metastable dis-

order giving rise to excess magnetization in the AF ground state upon FC. In the above discussion this effect was claimed to be connected with critical slowing down. If so, the  $\Delta\theta$  effect observed should sensitively decrease with decreasing cooling rate. Experiments towards this end are presently in preparation.

#### ACKNOWLEDGMENTS

We are grateful to V. Jaccarino for providing the excellent crystal used in the experiments and for discussions. Thanks are due to U. A. Leitão and W. Nitsche for valuable discussions and help with the experiments. It is a pleasure to thank T. Nattermann and J. Villain for elucidating discussions on the theoretical aspects of this work. D. P. B. gratefully acknowledges the hospitality during his stay with the Sonderforschungsbereich 166 of the Deutsche Forschungsgemeinschaft, which also provided financial support. Work at the University of California at Santa Cruz (UCSC) was partially supported by the Department of Energy under Grant No. DE-FG03-87ER45324.

- 
- <sup>1</sup>Y. Imry and S. K. Ma, *Phys. Rev. Lett.* **35**, 1399 (1975).  
<sup>2</sup>S. Fishman and A. Aharony, *J. Phys. C* **12**, L729 (1979).  
<sup>3</sup>For reviews, see R. J. Birgeneau, R. A. Cowley, G. Shirane, and H. Yoshizawa, *J. Stat. Phys.* **34**, 817 (1984); V. Jaccarino, in *Condensed Matter Physics—The Theodore D. Holstein Symposium*, edited by R. L. Orbach (Springer, New York, 1987); D. P. Belanger, *Phase Trans.* **11**, 53 (1988).  
<sup>4</sup>J. Z. Imbrie, *Phys. Rev. Lett.* **53**, 1747 (1984); J. Bricmont and A. Kupiainen, *ibid.* **59**, 1829 (1987).  
<sup>5</sup>J. Villain, *Phys. Rev. Lett.* **52**, 1543 (1984).  
<sup>6</sup>G. Grinstein and J. F. Fernandez, *Phys. Rev. B* **29**, 6389 (1984).  
<sup>7</sup>For a review, see T. Nattermann and J. Villain, *Phase Trans.* **11**, 5 (1988).  
<sup>8</sup>T. Nattermann, *Phys. Status Solid. B* **129**, 153 (1985).  
<sup>9</sup>T. Nattermann and I. Vilfan, *Phys. Rev. Lett.* **61**, 223 (1988).  
<sup>10</sup>M. Hagen, R. A. Cowley, S. K. Satija, H. Yoshizawa, G. Shirane, R. J. Birgeneau, and H. J. Guggenheim, *Phys. Rev. B* **28**, 2602 (1983).  
<sup>11</sup>G. S. Grest, C. M. Soukoulis, and K. Levin, *Phys. Rev. B* **33**, 7659 (1986).  
<sup>12</sup>H. Ikeda and K. Kikuta, *J. Phys. C* **17**, 1221 (1984).  
<sup>13</sup>U. A. Leitão and W. Kleemann, *Phys. Rev. B* **35**, 8696 (1987).  
<sup>14</sup>H. Yoshizawa and D. P. Belanger, *Phys. Rev. B* **30**, 5220 (1984).  
<sup>15</sup>U. A. Leitão, W. Kleemann, and I. B. Ferreira, the preceding paper, *Phys. Rev. B* **38**, 4765 (1988).  
<sup>16</sup>J. Villain, *J. Phys. (Paris)* **46**, 1843 (1985); D. S. Fisher, *Phys. Rev. Lett.* **56**, 416 (1986).  
<sup>17</sup>W. Kleemann, A. R. King, and V. Jaccarino, *Phys. Rev. B* **34**, 479 (1986).  
<sup>18</sup>A. R. King, J. A. Mydosh, and V. Jaccarino, *Phys. Rev. Lett.* **56**, 2525 (1986).  
<sup>19</sup>C. A. Ramos, A. R. King and V. Jaccarino, *Phys. Rev. B* **37**, 5483 (1988).  
<sup>20</sup>W. Nitsche and W. Kleemann, *Phys. Rev. B* **37**, 7680 (1988).  
<sup>21</sup>J. L. Cardy, *Phys. Rev. B* **29**, 505 (1984).  
<sup>22</sup>D. P. Belanger, A. R. King, and V. Jaccarino, *Solid State Commun.* **54**, 79 (1985).  
<sup>23</sup>J. Villain, in *Scaling Phenomena in Disordered Systems*, edited by R. Pynn and A. Skjeltorp (Plenum, New York, 1985), p. 423.  
<sup>24</sup>P. Z. Wong and J. W. Cable *Phys. Rev. B* **28**, 536 (1983).  
<sup>25</sup>D. P. Belanger, S. M. Rezende, A. R. King, and V. Jaccarino, *J. Appl. Phys.* **57**, 3294 (1985).